High Temp. Mater. Proc., Vol. **30** (2011), pp. 557–562 DOI 10.1515/HTMP.2011.113

Synthesis and Preparation of New Reinforced Montmorillonite Poly(amides-imides) Based on *N*-trimellitimido-4-amino Benzoic Acid

Khalil Faghihi,[1,*] **Meisam Shabanian**[2] **and Nooshin Bolhasani**[1]

[1] Polymer Research Laboratory, Department of Chemistry, Faculty of Science, Arak Branch, Islamic Azad University, Arak, Iran

[2] Young Researchers Club, Arak Branch, Islamic Azad University, Arak, Iran

Abstract. Two new samples of poly(amide-imide)-montmorillonite reinforced nanocomposites containing *N*-trimellitimido moiety in the main chain were synthesized by a convenient solution intercalation technique. Poly(amide-imide) (PAI) **5** as a source of polymer matrix was synthesized by the direct polycondensation reaction of *N*-trimellitimido-4-amino benzoic acid **3** with 4,4'-diamino diphenyl ether **4** in the presence of triphenyl phosphate (TPP), $CaCl_2$, pyridine and *N*-methyl-2-pyrrolidone (NMP). Morphology and structure of the resulting PAI-nanocomposite films **5a** and **5b** with 10 and 20% silicate particles were characterized by FTIR spectroscopy, X-ray diffraction (XRD) and scanning electron microscopy (SEM). The effect of clay dispersion and the interaction between clay and polymeric chains on the properties of nanocomposites films were investigated by using UV-vis spectroscopy, thermogravimetric analysis (TGA) and water uptake measurements.

Keywords. Montmorillonite nanocomposite, ether moiety, poly(amide-imide), thermal properties.

PACS®(2010). 81.05.Qk.

1 Introduction

Polymer-clay nanocomposites typically exhibited mechanical, thermal and gas barrier properties, which are superior to those of the corresponding pure polymers [1–9]. Unique properties of the nanocomposites are usually observed when the ultra fine silicate layers are homogenously dispersed throughout the polymer matrix at nanoscale. The uniform dispersion of silicate layers is usually desirable for maximum reinforcement of the materials. Due to the incompatibility of hydrophilic layered silicates and hydrophobic polymer matrix, the individual nanolayers are not easily separated and dispersed in many polymers. For this purpose, silicate layers are usually modified with an intercalating agent to obtain organically modified clay prior to use in nanocomposite formation [10, 11]. Also aromatic polyimides are well recognized as a class of high performance materials due to their remarkable thermal and oxidative stabilities and excellent electrical and mechanical properties for long time periods of operation [10–12]. Unfortunately, strong interaction between polyimide chains and their rigid structure make them intractable. Poor thermoplastic fluidity and solubility are the major problems for wide application of polyimides. Thus, to overcome these processing problems various approaches have been carried out by incorporating flexible units such as –NHCO–, –O–, and $–SO_2–$, and some of which are commercialized [13–15]. Among them, polyamide-imide (PAI) is the most successful material, which combines the advantages of high-temperature stability and processability [16–22]. In this article two PAI-nanocomposite films with 10 and 20% silicate particles containing chiral *N*-trimellitimido-4-amino benzoic acid moiety in the main chain was prepared by using a convenient solution intercalation technique.

2 Experimentals

2.1 Materials

Trimellitic anhydride, 4-amino benzoic acid, 4,4'-diamino diphenyl ether, acetic acid, triphenyl phosphate (TPP), $CaCl_2$, pyridine and *N*-methyl-2-pyrrolidone (NMP) were purchased from Merck Chemical Company and used without previous purification. The organic modifiers and the interlayer distance of the clays are shown in Table 1 to account the structural modifications of the functional points.

2.2 Measurements

^{1}H-NMR spectrum was recorded on a Bruker 300 MHz instrument (Germany). Fourier transform infrared (FTIR)

* **Corresponding author:** Khalil Faghihi, Polymer Research Laboratory, Department of Chemistry, Faculty of Science, Islamic Azad University, Arak Branch, Arak, Iran;
E-mail: k-faghihi@araku.ac.ir.

Received: February 12, 2011. Accepted: March 10, 2011.

Type of clay	Organic modifier	Concentration of organic modifier [meq/100 g clay]	Interlayer distance (nm)
Cloisite® 20A	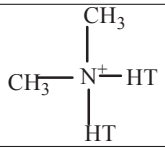	95	1.77

Table 1. Organic modifiers and Interlayer Distance of the clays.

spectra were recorded on Galaxy Series FTIR 5000 spectrophotometer (England). Vibration transition frequencies were reported in wave number ($cm^{-1} = 10^{-2}\ m^{-1}$). UV-visible spectra were recorded at 298 K in the 250–700 nm spectral regions with a Perkin Elmer Lambda 15 spectrophotometer in NMP solution using cell lengths of 1 cm. Thermal Gravimetric Analysis (TGA and DTG) data were taken on a Mettler TA4000 System under N_2 atmosphere at a rate of 10 K/min. The morphology of nanocomposite film was investigated on Cambridge S260 scanning electron microscope (SEM).

2.3 Monomer Synthesis

N-trimellitimido-4-amino benzoic acid **3** was prepared according to a typical procedure was shown in scheme 1 [23].

2.4 Polymer Synthesis

Into a 100 mL round bottomed flask were placed a mixture of *N*-trimellitimido-4-amino benzoic acid **3** (0.002 mol), 4,4'-diamino diphenyl ether **4** (0.002 mol), 0.60 g of calcium chloride, 1.0 mL of triphenyl phosphite, 1.0 mL of pyridine and 4.0 mL NMP. The mixture was heated for 1 h at 333K, 2 h at 363 K and then refluxed at 403 K for 8 h until a viscous solution was formed. Then it was cooled to room temperature and 30 mL of methanol was added to reaction mixture. The precipitate was formed, filtered off and washed with methanol. The resulting polymers 5 were dried under vacuum. The inherent viscosity of this soluble PA **5** was 1.06 dL/g.

2.5 PAI-nanocomposite Synthesis 5a and 5b

PAI-nanocomposites **5a** and **5b** were produced by solution intercalation method; in two different amounts of organoclay particles (10 and 20 mass %) were mixed with appropriate amounts of PAI solution in *N*-methyl-2-pyrrolidone (NMP) to yield particular nanocomposite concentrations. To control the dispersibility of organoclay in poly(amide-imide) matrix, constant stirring was applied at 298 K for 24 h. Nanocomposite films were cast by pouring the solutions for each concentration into Petri dishes placed on a leveled surface followed by the evaporation of solvent at 353 K (= 80°C) for 12 h. Films were dried at 363 under vacuum to a constant weight. Scheme **1** show the flow sheet diagram and synthetic scheme for PAI-nanocomposites film **5a** and **5b**.

2.6 The Water Absorption Analysis

The water absorption of PAI-nanocomposite films was carried out using a procedure under ASTM D570-81 [24]. The films were dried in a vacuum oven at 353 K to a constant weight and then weighed to get the initial weight (W_0). The dried films were immersed in deionized water at 283 K. After 24 h, the films were removed from water and then they were quickly placed between sheets of filter paper to remove the excess water and films were weighed immediately. The films were again soaked in water. After another 24 h soaking period, the films were taken out, dried and weighed for any weight gain. This process was repeated again and again till the films almost attained the constant weight. The total soaking time was 168 h and the samples were weighed at regular 24 h time intervals to get the final weight (W_f). The percent increase in weight of the samples was calculated by using the formula $(W_f - W_0)/W_0$.

3 Results and Discussion

3.1 Monomer Synthesis

N-trimellitimido-4-amino benzoic acid **3** was synthesized from the reduction of p-amino benzoic acid **2** by trimellitic anhydride **1** in a basic solution (Figure 1).

3.2 Polymer Synthesis

Poly(amide-imide)s **5** was synthesized by the direct solution polycondensation reaction of an equimolar mixture of diacid 3 (Figure 2), an equimolar mixture of diamine **4** by using triphenyl phosphate (TPP) and pyridine as condensing agents (Scheme 2). PAI **5** was obtained in good yield (92%) and inherent viscosity (1.06 dL/g). The structure of resulting polymer **5** was confirmed as PAI by using FTIR spectroscopy and elemental analyses. The resulting polymer have absorption band between 1776 and 1665 cm^{-1} ($cm^{-1} = 10^{-2}\ m^{-1}$). due to imide and amide carbonyl

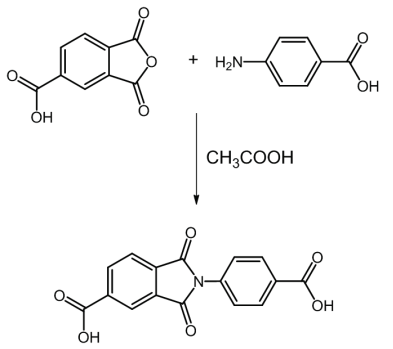

Figure 1. Synthetic route of *N*-trimellitimido-4-amino benzoic acid **3**.

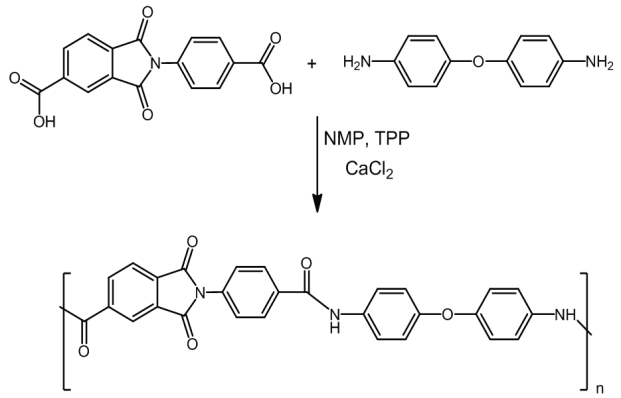

Figure 2. Synthetic route of PAI **5**.

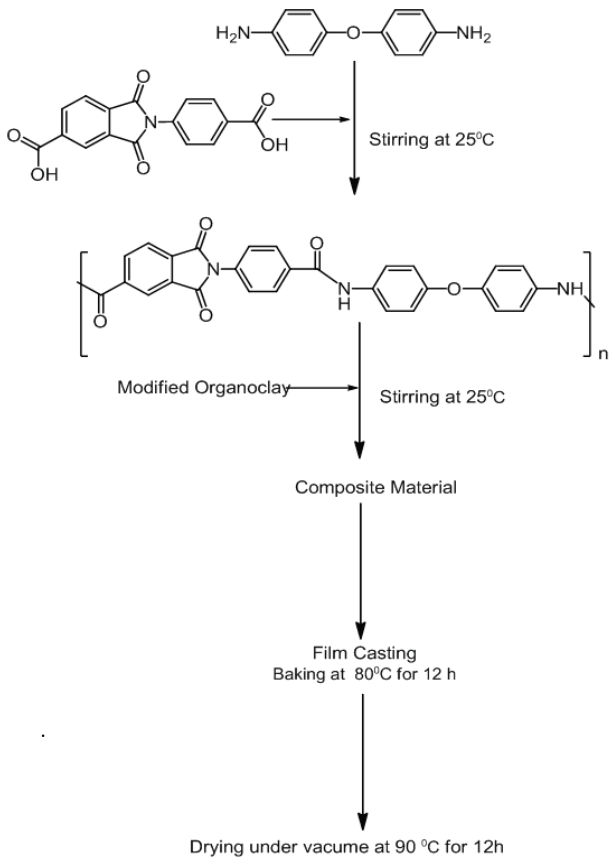

Figure 3. Flow sheet diagram for the synthesis of PAI-nanocomposites film **5a** and **5b**.

groups. Absorption bands around 1384 cm^{-1} and 719 cm^{-1} demonstrated the presence of the imide heterocyclic absorption in these polymers. Also absorption band of amide group appeared at 3338 cm^{-1} (N–H stretching). The elemental analysis value of the resulting polymer was in good agreement with the calculated values for the proposed structure.

3.3 PAI-nanocomposite Films

PAI-nanocomposite films were transparent and yellowish brown in color. The incorporation of organoclay changed the color of films to dark yellowish brown. Moreover, a decrease in the transparency was observed at higher clay contents. Figure 3 shows the flowsheet diagram and synthetic scheme for PAI-nanocomposites film **5a** and **5b**.

3.4 Characterization

3.4.1 FT-IR Spectroscopy Analyses

FT-IR spectroscopy spectra of PAI-nanocomposite films **5a** and **5b** showed the characteristic absorption bands of the Si-O and Mg-O moieties at 1038, 515 and 465 cm^{-1} respectively. The incorporation of organic groups in PAI-nanocomposite films was confirmed by the presence of peaks at 1770, 1720, 1390, 725 (imide rings) and 1680 (amide carbonyl group) (Figure 4).

3.4.2 X-ray Diffraction Analysis

Figure 5 shows the XRD patterns of PAI-nanocomposite films **5a** and **5b** containing 10 and 20 mass % of silicate particles. The result reveals an increased d-spacing from 1.00 nm (8.78°) of Na-MMT to 1.49 nm (5.92°) of PAI-nanocomposite film (10 mass %) and (5.92°) of PAI-nanocomposite film (20 mass %). These results indicated significant expansion of the silicate layer after insertion PAI chains. The shift in the diffraction peaks PAI-nanocomposite films confirms that intercalation has been taken place. This is direct evidence that PAI-nanocomposites have been formed as the nature of intercalating agent also affects the organoclay dispersion in the polymer matrix. Usually there are two types of nnaocomposites depending upon the dispersion of clay particles. The first type is an intercalated polymer clay nanocomposite, which consists of well ordered multi layers of polymer chain and silicate layers a few nanometers thick. The sec-

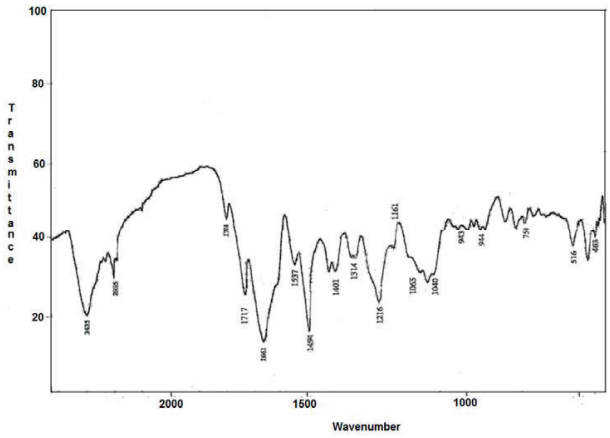

Figure 4. FTIR spectrum in unit cm^{-1} of PAI-nanocomposite films **5a**.

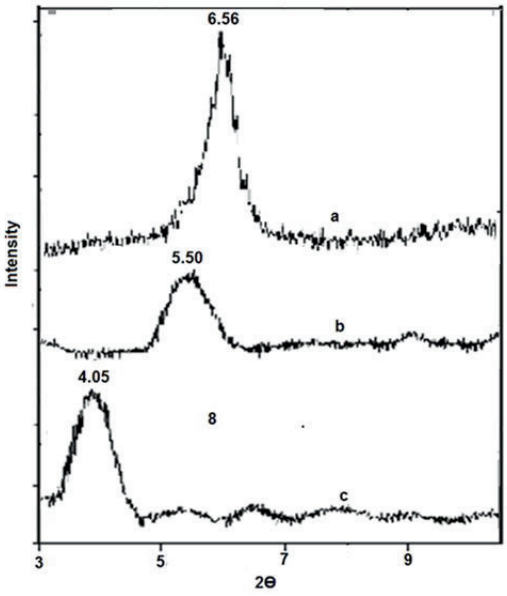

Figure 5. X-ray diffraction patterns of Organoclay (**a**), PAI-nanocomposite films **5a (b)** and **5b (c)**.

ond type is an exfoliated polymer-clay nanocomposite, in which is there is a loss of ordered structures due to the extensive penetration of polymer chain into the layer silicate. Such part would not produce distinct peaks in the XRD pattern [25]. In our PAI- nanocomposite films there are coherent XRD signal at 5.92° and 5.92° related to 10 and 20 mass % nanocomposite films respectively (Figure 5).

3.4.3 Scanning Electron Microscopy

The surface morphology of the PAI-nanocomposite films prepared by solution intercalation technique is compared by SEM analyses. Figures 4 and 5 show the morphological images of 10 and 20 mass % nanocomposite films respectively. The SEM images show that PAI matrix has a smooth morphology, where as the PAI matrix has amorph morphology. Also SEM micrographs of PAI-nanocomposite containing 10 and 20 mass % clay platelets were uniformly distributed without agglomeration (Figure 6).

3.4.4 Optical Clarity of PAI-nanocomposite Films

Optical clarity of PAI-nanocomposite films containing 10 and 20 mass % clay platelets and neat PAI was compared by UV-vis spectroscopy in the region of 300–800 nm.

Figure 7 show the UV-vis transmission spectra of pure PAI and PAI-nanocomposite films containing 10 and 20 mass % clay platelets. These spectra show that the UV-visible region (250–800 nm) is affected by the presence of the clay particles and exhibiting low transparency reflected to the primarily intercalated composites. Results shows that the optical clarity of PAI-nanocomposite films system is significantly lower the neat PAI system.

3.4.5 Thermogravimetric Analysis

The thermal properties of PAI-nanocomposite films containing 10 and 20 mass % clay platelets and neat PAI were investigated by using TGA and DTG in nitrogen atmosphere at a rate of heating of 10 K/min, and thermal data are summarized in Table 2. These samples exhibited good resistance to thermal decomposition, up to 425–446 K, in nitrogen, and began to decompose gradually above this temperature. T_5 for these polymers ranged from 425–446 K and T_{10} for them ranged from 430–478 K, and residual weights at 873 K ranged from 48 and 63 % in nitrogen. Incorporation of organoclay into the PAI matrix also enhanced the thermal stability of the nanocomposites. Figure 8 shows the TGA thermograms of PAI-nanocomposites under nitrogen atmosphere. Thus, we can speculate that interacting PAIs chains between the clay layers serve to improve the thermal stability of nanocomposites. The addition of organoclay in polymeric matrix can significantly improve the thermal stability of PAI.

3.4.6 Water Absorption Measurements

The PAI under investigation contains polar and cyclic imide rings and also polar amide groups in the backbone that have the tendency to uptake water through hydrogen bonding. Thus water absorption measurements become necessary for neat PAI **5** and PAI-nanocomposite films **5a** and **5b** and data are shown in Table 2. In the water permeability studies, we found that the incorporation of clay platelets into PAI matrix results in a decrease of water uptake relative to pure PAI by forming the tortuous path of water permeant. Water permeability depends on length, orientation and degree

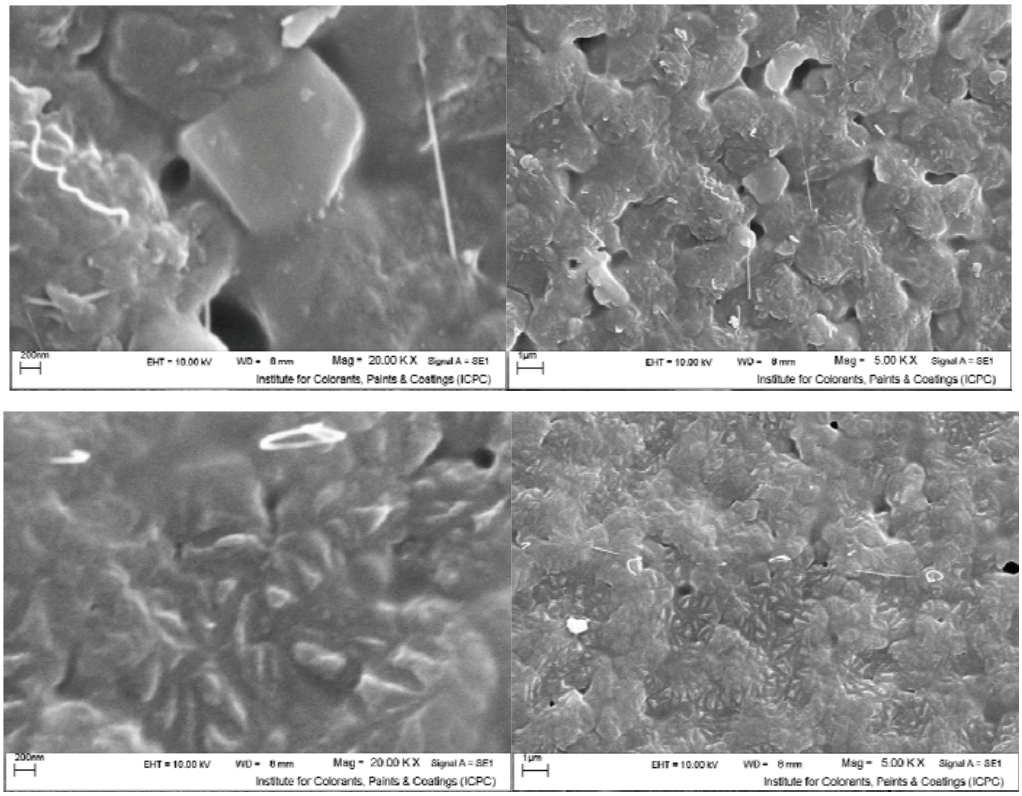

Figure 6. Scanning electron micrographs of PAI-nanocomposite films **5a (a)** and **5b (b)**.

Polyimide	T_5 (K)[a]	T_{10} (K)[b]	Char Yield[c]	Water uptake (%)
5	425	430	48	7/57
5a	443	471	54	5/04
5b	446	205	63	0/16

[a,b] Temperature at which 5% and 10% mass loss was recorded by TGA at heating rate of 10 K/min in N_2 respectively.

[c] Percentage weight of material left undecomposed after TGA analysis 873 K.

Table 2. Thermal behaviors and Water uptake of neat PAI **5** and PAI-nanocomposite films **5a** and **5b**.

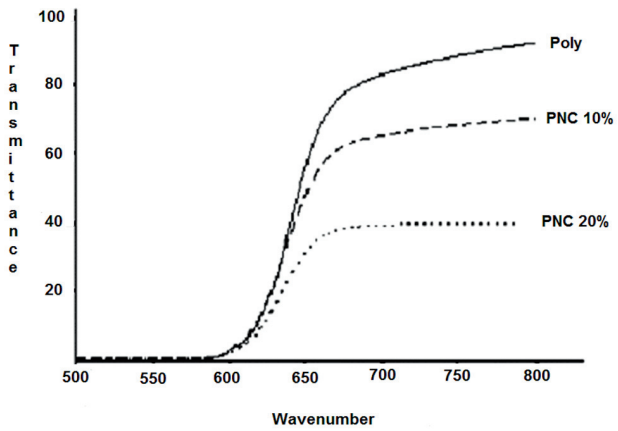

Figure 7. Uv-vis spectra in unit of cm^{-1} of PAI **5**, PAI-nanocomposite films **5a** and **5b**.

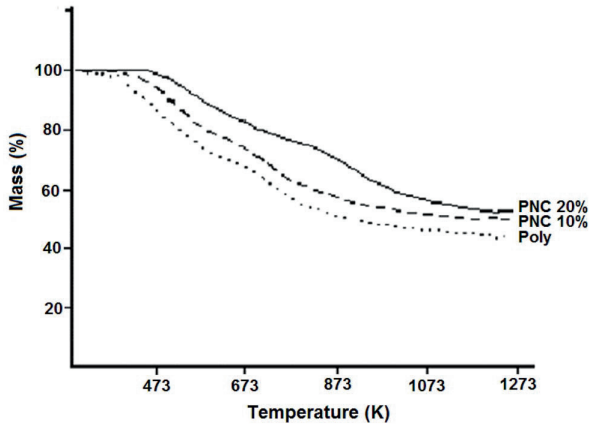

Figure 8. TGA thermograms of neat PAI **5** and PAI-nanocomposite films **5a** and **5b**.

of delamination of layered silicate [26]. It should be noted that a further increase in clay concentration resulted in an enhanced barrier property of nanocomposites which may be attributed to the plate-like clays that effectively increase the length of the diffusion pathways, as well as decrease the water permeability.

4 Conclusions

The PAI-nanocomposites were successfully prepared using solution intercalation method. The structure and the uniform dispersion of organoclay throughout the PAI matrix were confirmed by FTIR, XRD and SEM analyses. The optical clarity and water absorption property of PAI-nanocomposites were decreased significantly with increasing the organoclay contents in PAI matrix. On the contrary the thermal stability of PAI-nanocomposites were increased significantly with increasing the organoclay contents in PAI matrix. The enhancements in the thermal stability of the nanocomposites films **5a** and **5b** caused by introducing organoclay may be due to the strong interactions between polymeric matrix and organoclay generating well intercalation and dispersion of clay platelets in the PAI matrix.

References

[1] E. P. Giannelis, *Adv. Mater.*, **8** (1996), 29–35.

[2] Y. Yano, A. Usuki, T. Kurauchi and O. Kamigato, *J. Polym. Sci. Part A: Polym. Chem.,* **31** (1993), 2493–2498.

[3] S. Zulfiqar, Z. Ahmad, M. Ishaq, S. Saeed and M. I. Sarwar, *J. Mater. Sci.,* **42** (2007), 93–100.

[4] M. Sikka, L. N. Cerini, S. S. Ghosh and K. I. Winey, *J. Polym. Sci. Part B: Polym. Phys.*, **34** (1996), 1443–1449.

[5] R. Xu, E. Manias, A. J. Snyder and J. Runt, *Macromolecules*, **34** (2001), 337–339.

[6] A. Kausar, S. Zulfiqar, S. Shabbir, M. Ishaq and M. I. Sarwar, *Polym. Bull.*, **59** (2007), 457–468.

[7] N. Bibi, M. I. Sarwar, M. Ishaq and Z. Ahmad, *Polym. Polym. Compos.*, **15** (2007), 313–319.

[8] S. Zulfiqar and M. I. Sarwar, *Scr. Mater.*, **59** (2008), 436–439.

[9] T. D. Fornes, P. J. Yoon, D. L. Hunter, H. Keskkula and D. R. Paul, *Polymer,* **43** (2002), 5915–5933.

[10] G. M. Chen, Y. M. Ma and Z. N. Qi, *J. Appl. Polym. Sci.,* **77** (2000), 2201–2205.

[11] Y. Yano, A. Usuki, T. Kurauchi and O. Kamigato, *J. Polym. Sci. Part A: Polym. Chem.,* **31** (1993), 2493–2498.

[12] Kh. Faghihi, F. Shabani and M. Shabanian, *J. Macromol. Sci. Part A Pure Appl. Chem.*, **48** (2011), 381–386.

[13] M. K. Ghosh and K. L. Mittal, *Polyimide: Fundamental and Applications,* Dekker: New York, 1996.

[14] D. J. Liaw and B. Y. Liaw, *Polymer*, **42** (2001), 839–845.

[15] Kh. Faghihi and M. Shabanian, *Macromol. Res.,* **18** (2010), 1148–1153.

[16] Q. Zhang, S. Li, W. Li and S. Zhang, *Polymer*, **48** (2007), 6246–6253.

[17] Q. Zhang, G. Chen, S. Zhang, *Polymer*, **48** (2007), 2250–2256.

[18] A. Saxena, V. L. Rao, P. V. Prabhakaran and K. N. Ninan, *Eur. Polym. J.* **39** (2003), 401–405.

[19] C. P. Yang, Y. P. Chen and E. M. Woo, *Polymer*, **45** (2004), 5279–5293.

[20] D. J. Liaw and W. H. Chen, *Polym. Degrad. Stab.*, **91** (2006), 1731–1739.

[21] Kh. Faghihi, M. Shabanian and M. Hajibeygi, *Macromol. Res.,* **17** (2009), 912–918.

[22] Kh. Faghihi, M. Hajibeygi and M. Shabanian, *Macromol. Res.,* **17** (2009), 739–745.

[23] S. Mallakpour, A. R. Hajipour and S. Habibi, *J. Appl. Polym. Sci.,* **80** (2001), 1312–1318.

[24] S. Zulfiqar and M. I. Sarwar, *J. Incl. Phenom. Macrocycl. Chem.*, **62** (2008), 353–361.

[25] P. S.G. Krishnan, A. E. Wisanto, S. Osiyemi, C. Ling, *Polym. Inter.*, **56** (2007), 787–795.

[26] R. K. Bharadwaj, *Macromolecules,* **34** (2001), 9189–9192.